Analysis of radio frequency heating induced by a coronary stent at 7.0 T

Davide Santoro[1], Alexander Müller[1,2], Lukas Winter[1], Wolfgang Renz[1,3], Andreas Grässl[1], Celal Özerdem[1], Valeriy Tkachenko[4], Jeanette Schulz-Menger[4], and Thoralf Niendorf[1,4]

[1]Berlin Ultra-High Field Facility (BUFF), Max Delbrück Center for Molecular Medicine (MDC), Berlin, Germany, [2]Department of physics, Humboldt-Universität zu Berlin, Berlin, Germany, [3]Siemens Healthcare, Erlangen, Germany, [4]Working Group on Cardiovascular Magnetic Resonance, Experimental and Clinical Research Center (ECRC), Medical University Berlin, Charité Campus Buch, Berlin, Germany

Introduction: The signal-to-noise ratio (SNR) advantages of ultrahigh field MRI hold the promise to enhance spatial and temporal resolution [1,2,3]. Such improvements could find an ever-growing number of applications in cardiovascular MR (CMR), including the characterization of ischemic disorders on the myocardial tissue level through mapping microstructures, and parametric imaging [4]. However, intracoronary stents used for treatment of coronary artery disease (CAD) are currently considered to be contra-indications for CMR at 7.0 T. The antenna effect due to the presence of a metallic implant in combination with RF wave lengths could lead to high RF power deposition at 7.0 T, which will induce local heating and may potentially cause myocardial tissue damage, influence coagulation or endothelial function. For all these reasons it is essential to carefully assess RF induced heating in coronary stents commonly used in percutaneous coronary intervention. To meet this goal this work examines RF induced heating of a copper tube and of a coronary stent in agarose phantoms using electromagnetic field (EMF) simulations, fiber optic temperature measurements and MR thermometry at 7.0 T.

Methods: An eight rung highpass circular polarized birdcage RF coil with an inner diameter of 20cm was build to provide RF power which is beyond that of clinical standards. Cylindrical phantoms (V=600ml, Ø=13.5cm, 4% agarose, NaCl-concentration = 5g/l, CuSo4-concentration=1g/l) were setup to match the conductivity of heart muscle tissue [5] with σ=1.2 S/m and to have a permittivity ε_r=78 A cobalt chromium alloy coronary stent with l=27 mm and Ø=4 mm (Biotronik, Bülach, CH) was placed into one phantom; one copper pipe (l=4cm, Ø=5mm) was placed into another phantom and a third agarose phantom was used as a control. EMF simulations based on a FDTD method (CST software, Darmstadt, Germany) were performed using the design and geometry of the birdcage coil and of the phantoms. MR thermometry using the proton resonance frequency method (PRF) [6,7] was performed to monitor temperature changes in the phantom experiments. To correct for temperature induced conductivity changes, two gradient echoes were acquired [8,9]. For validation, temperature was measured in different locations of the phantom using a fiber optics system (OpSens, Quebec, CA). RF heating was achieved by repeating the single pulse experiment, with FA=200° (Ref V=194V, τ=500µs, TR=11.4ms, Averages=800, TA=20minutes). Every 20 minutes of RF heating, a 3D-GRE image was acquired (TR=10ms, $TE_{1,2}$=2.04/6.12ms, FA=15°, FOV=15x15x10cm^3, TA= 14s). The experiments were repeated for 1 hour for each phantom.

Results: The simulations shown in Fig. 1 were used to determine the position with the strongest E-field in the control phantom: this induce a simulated ΔT pattern as shown in Fig.1, bottom. The copper tube and the stent were placed in the bottom left corner to provide the worst case scenario for coupling and RF heating [10]. Fig.2 shows the agreement among fiber optics measurements and MR thermometry in the control phantom with an accuracy of ±1°C. Figure 4 shows the 3D temperature changes maps acquired with MR thermometry in the control experiment and in the one with the coronary stent. The distribution of the temperature increase is similar with no strong change induced by the stent. To confirm this, the map of the control phantom has been subtracted from that of the phantoms with the copper tube and the stent, as shown in Fig. 5 (only the partitions with the highest heating are shown); this shows only the additional heating induced by the antenna effect in a metallic object and it is limited to a 10% increase only. However the results are limited to regions where the induced MR artifacts do not prevent an accurate measure of the T maps.

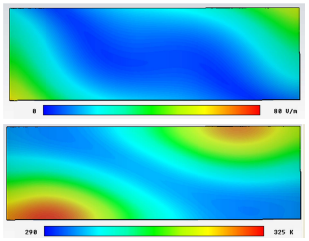

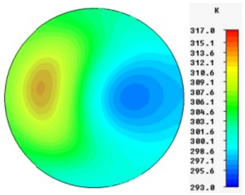

Fig. 1. Simulation of the E-field (top left, in V/m) in the control virtual phantom induced by RF heating with the birdcage coil (central axial partition) and the corresponding temperature simulation (bottom left, starting temperature 292 K). A coronal view at 2cm from the bottom is show on the right. The stationary solution is displayed for the case of a continuous RF irradiation with a power of 50W.

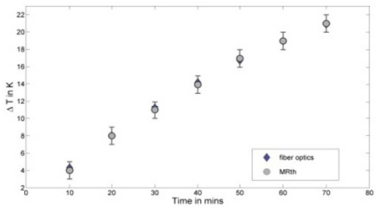

Fig. 2. Temperature time course measured with fiber optics probes and MR thermometry (averaged, near probe locations) for the control phantom for about 70 mins of RF heating.

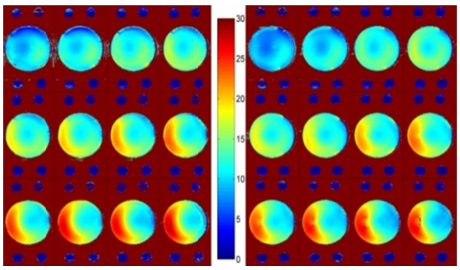

Fig. 3. 3D ΔT maps (in °C) obtained with MR thermometry in the control phantom (left) and with the coronary stent (right) after 60 mins of RF heating. Four oil references were placed next to the phantoms.

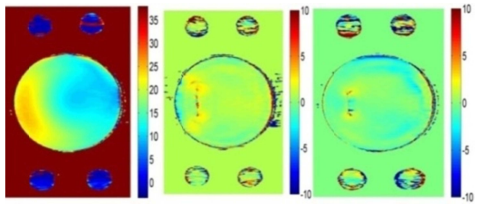

Fig. 4. **Left**: ΔT map (in °C) of the agarose gel control phantom after 1 hour of RF heating **Centre**: Difference of the ΔT maps of the phantom with the copper tube and the control phantom, after 1 hour of RF heating. **Right**: Difference of the ΔT maps of the phantom with the coronary stent and the control phantom, after 1 hour of RF heating.

Discussion: Our results show an overall agreement between the simulated electric field in a virtual phantom and the temperature maps derived from phantom experiments using MR thermometry. The temperature changes induced by the strong RF heating applied for 1 hour, reach about +25 °C in some areas of the phantom, however the increase due to the metallic wire or the coronary stent are only about 4 °C. For the chromium alloy coronary stent no extra hot spots were evident in the 3D temperature maps in our setup. Further simulations of the E-field with an accurate model of the stent, could provide information about possible heating in the close proximity of the surface, where MR thermometry cannot provide information.

References: **[1]** Hecht EM et al., Magn Reson Imaging Clin N Am 15:449–465, 2007. **[2]** Niendorf,T et al., European Radiology (2010-07-31). **[3]** von Knobelsdorff-Brenkenhoff et al., European Radiology (2010-07-17). **[4]** Mainero et al., Neurology 73:941–948, 2009. **[5]** Gabriel, C, DTIC Document, 1996. **[6]** Ishihara Y et al., MRM 34:814–823, 1995. **[7]** Gellermann J et al., Int. J. Hyperthermia, 21(6): 497–513, September 2005. **[8]** Rieke V, Magn. Reson. Imaging, 27: 376-390, 2007. **[9]** Wonneberger U, J. Magn. Reson. Imaging, 31: 1499-1503, 2010. **[10]** Nordbeck P, et al., MRM, 60-312/319, 2008.